

# Effect of Cholesterol on the Solubilization Site and the Photoionization Efficiency of Chlorophyll *a* in Dipalmitoylphosphatidylcholine Vesicle Solutions As Studied by Electron Spin Resonance and Optical Absorption Spectroscopies

Ichiro Hiromitsu and Larry Kevan\*

Contribution from the Department of Chemistry, University of Houston, Houston, Texas 77004.  
Received September 17, 1986

**Abstract:** Electron spin resonance (ESR) and optical absorption studies are carried out to investigate the solubilization site and the photoionization efficiency of chlorophyll *a* (Chla) in DL- $\alpha$ -dipalmitoylphosphatidylcholine (DPPC) vesicles due to varying concentration of cholesterol. With an increase in the cholesterol concentration, the optical absorption intensity of Chla decreases in liquid vesicle solutions, indicating that the local light intensity inside the vesicle decreases. Photoionization efficiencies of Chla in frozen vesicle solutions with and without potassium ferricyanide, a lipophobic electron scavenger, decrease with the cholesterol addition, while no effect of added cholesterol is seen in electron-transfer efficiency from photoexcited Chla to *p*-benzoquinone, a lipophilic electron scavenger, in liquid vesicle solution. Paramagnetic dipolar interaction between photoproduced Chla cation and added ferricyanide ion becomes weaker with cholesterol addition in frozen vesicle solutions. It is concluded that both Chla and *p*-benzoquinone move deeper into the vesicle bilayer when cholesterol is added because of an increase in the internal fluidity or alkyl chain straightening of the bilayer.

Photoinduced charge separation of photosensitive solutes and the subsequent charge transport in organized molecular assemblies such as micelles, vesicles, and planar bilayers have been typical models for artificial photosynthetic reactions.<sup>1-10</sup> In order to achieve light energy utilization with such systems, it is necessary to control the net charge separation efficiency which is largely determined by the rate of back reactions after the initial charge separation. The net charge separation efficiency is strongly affected by structural factors such as the location of the electron donors and acceptors relative to the micelle or bilayer surface, the surface charge distribution on the micelle or bilayer, and the degree of interaction between water and the micelle or bilayer surfaces. It has been shown that these structural factors are controllable by changing counterions,<sup>11,12</sup> headgroups,<sup>13-16</sup> or hydrocarbon tail length<sup>17</sup> of the amphiphiles or by adding salts<sup>18-20</sup> or slightly water-soluble alcohols.<sup>21,22</sup> The present study shows

another way to control vesicle structure so as to affect photoionization efficiency by adding cholesterol. This is somewhat analogous to the addition of slightly water-soluble alcohols to micelles.

Cholesterol is an important constituent of many natural membranes having a function of controlling the hydrocarbon chain fluidity of the lipid components of membranes.<sup>23,24</sup> It is known that cholesterol can enter into phospholipid bilayers to a level of one molecule of cholesterol per molecule of the phospholipid<sup>23,25</sup> without destroying the bilayer structure. In the present study, cholesterol is added to DPPC vesicles containing Chla, and its effects on the solubilization site and the photoionization efficiency of Chla are investigated by ESR and optical absorption spectroscopies. Three types of DPPC vesicle solutions are prepared: (1) with no electron scavenger, (2) with *p*-benzoquinone (PBQ), a lipophilic electron scavenger inside the vesicle bilayer, and (3) with potassium ferricyanide ( $K_3Fe(CN)_6$ ), a lipophobic electron scavenger residing outside the vesicle. The photoionization of Chla in these systems without cholesterol has been studied in this laboratory by Ohta and Kevan at 77 K.<sup>26</sup> They observed the formation of Chla cation radical (Chla<sup>+</sup>) at 77 K in system (1) for the first time. In the present study Chla is photoexcited both in liquid vesicle solutions at room temperature and in frozen vesicle solutions at 77 K.

Optical absorption studies of Chla, PBQ, and  $K_3Fe(CN)_6$  in liquid vesicle solutions show that the absorbance must be corrected for the local light intensity penetrating the vesicle wall. A decrease in the local light intensity at the Chla site within the vesicle is found by cholesterol addition. From ESR measurements of paramagnetic relaxation times of Chla<sup>+</sup> in system (3) and of photoionization yields in systems (1)-(3), it is deduced that both Chla and PBQ move deeper into the vesicle bilayer when cholesterol is added, presumably because of an increase in the fluidity

- (1) Grätzel, M.; Thomas, J. K. *J. Phys. Chem.* **1974**, *78*, 2248.
- (2) Fendler, J. H. *Acc. Chem. Res.* **1980**, *13*, 7.
- (3) Calvin, M. *Photochem. Photobiol.* **1983**, *37*, 349.
- (4) Narayana, P. A.; Li, A. S. W.; Kevan, L. *J. Am. Chem. Soc.* **1981**, *103*, 3603.
- (5) Ohta, N.; Kevan, L. *J. Phys. Chem.* **1985**, *89*, 3070.
- (6) Krakover, T.; Ilani, A.; Mauzerall, D. *Biophys. J.* **1981**, *35*, 93.
- (7) Ilani, A.; Mauzerall, D. *Biophys. J.* **1981**, *35*, 79.
- (8) Ilani, A.; Liu, T. M.; Mauzerall, D. *Biophys. J.* **1985**, *47*, 679.
- (9) Liu, T. M.; Mauzerall, D. *Biophys. J.* **1985**, *48*, 1.
- (10) Woodle, M. C.; Mauzerall, D. *Biophys. J.* **1986**, *50*, 431.
- (11) Szajdzinska-Pietek, E.; Maldonado, R.; Kevan, L.; Jones, R. R. M.; Coleman, M. J. *J. Am. Chem. Soc.* **1985**, *107*, 784.
- (12) Jones, R. R. M.; Maldonado, R.; Szajdzinska-Pietek, E.; Kevan, L. *J. Phys. Chem.* **1986**, *90*, 1126.
- (13) Li, A. S. W.; Kevan, L. *J. Am. Chem. Soc.* **1983**, *105*, 5752.
- (14) Plonka, A.; Kevan, L. *J. Phys. Chem.* **1985**, *89*, 2087.
- (15) Fang, Y.; Tollin, G. *Photochem. Photobiol.* **1983**, *38*, 429.
- (16) Fang, Y.; Tollin, G. *Photochem. Photobiol.* **1984**, *39*, 685.
- (17) Narayana, P. A.; Li, A. S. W.; Kevan, L. *J. Am. Chem. Soc.* **1982**, *104*, 6502.
- (18) Maldonado, R.; Kevan, L.; Szajdzinska-Pietek, E.; Jones, R. R. M.; *J. Chem. Phys.* **1984**, *81*, 3958.
- (19) Plonka, A.; Kevan, L. *J. Chem. Phys.* **1985**, *82*, 4322.
- (20) Hiromitsu, I.; Kevan, L. *J. Phys. Chem.* **1986**, *90*, 3088.
- (21) Szajdzinska-Pietek, E.; Maldonado, R.; Kevan, L.; Jones, R. R. M. *J. Am. Chem. Soc.* **1985**, *107*, 6467.

- (22) Szajdzinska-Pietek, E.; Maldonado, R.; Kevan, L.; Jones, R. R. M. *J. Colloid Interface Sci.* **1986**, *110*, 514.
- (23) Jain, M. K. In *Current Topics in Membranes and Transport*; Bronner, F., Kleinzeller, A., Eds.; Academic Press: New York, 1975; Vol. 6, p 1.
- (24) Chapman, D. In *Membrane Fluidity in Biology*; Aloia, R. C., Ed.; Academic Press: New York, 1983; Vol. 2, p 15.
- (25) Tanford, C. In *The Hydrophobic Effect*; Wiley-Interscience: New York, 1980; p 121.
- (26) Ohta, N.; Kevan, L. *J. Phys. Chem.* **1985**, *89*, 3070.

or alkyl chain straightening inside the bilayer.

### Experimental Section

Chla was extracted from fresh spinach leaves by the usual method of column chromatography on sugar.<sup>27</sup> The purity of Chla was estimated spectrophotometrically as  $96 \pm 4\%$  by using the literature value of its extinction coefficient ( $8.63 \times 10^4 \text{ M}^{-1} \text{ cm}^{-1}$ ) in diethyl ether at 660 nm.<sup>27</sup> DPPC and cholesterol were purchased from Sigma Chemical Co., PBQ from Aldrich Chemical Co., and  $\text{K}_3\text{Fe}(\text{CN})_6$  from Baker Chemical Co. A buffer solution was prepared with sodium phosphate from Fisher Scientific Co., sodium pyrophosphate from Aldrich Chemical Co., and sodium ethylene diamine tetraacetate (EDTA) from Alfa Products. Cholesterol was recrystallized from absolute ethanol. PBQ was sublimed and stored below  $0^\circ\text{C}$ . The other chemicals were used without further purification.

DPPC vesicle solutions of Chla were prepared by sonication as described previously.<sup>26,28</sup> Chloroform solutions of DPPC containing Chla and cholesterol were evaporated at  $50\text{--}55^\circ\text{C}$  for 2 h. The resulting films were sonicated in aqueous buffer solution, which had been deaerated beforehand by  $\text{N}_2$  bubbling for 15 min, with a Fisher Model 300 sonic dismembrator operated at a power level of 4.5 db with a 4 mm o.d. microtip for 1 h at  $50\text{--}55^\circ\text{C}$ . Undispersed lipids and Chla were removed by filtration. A buffer solution containing 0.1 M sodium phosphate, 0.1 M sodium pyrophosphate, and 1 mM EDTA in triply distilled water was adjusted to pH 7.0 with sulfuric acid.  $\text{K}_3\text{Fe}(\text{CN})_6$  was added to the vesicle solutions after sonication. PBQ was dissolved in the starting chloroform solutions of DPPC, cholesterol, and Chla prior to evaporation. Since degradation of PBQ was observed after the evaporation and the sonication at  $50\text{--}55^\circ\text{C}$ , vesicle solutions containing PBQ were prepared by evaporation at room temperature for 3 h and sonication at  $50\text{--}55^\circ\text{C}$  for 30 min. The final amounts of DPPC, Chla, PBQ, and  $\text{K}_3\text{Fe}(\text{CN})_6$  were 45, 1.5, 7, and 10 mM, respectively, unless otherwise noted. The amount of cholesterol was either 0, 10, 20, 35, or 50 mol % relative to the amount of DPPC. The vesicle solutions were sealed into  $2 \times 3$  mm diameter Suprasil quartz tubes and 75 mL (1-mm i.d.) Pyrex micropipets for photoirradiations at 77 K and at room temperature, respectively. The micropipets did not give any ESR signal from the photoirradiation. The entire sample preparation was carried out under nitrogen gas atmosphere and under minimal light.

Photoirradiation was carried out by using a Cermax 300 W xenon lamp with a power supply from ILC Technology. The light was passed through a 10-cm water filter and a Corning 2412 or 5030 glass filter for red-light ( $\gamma_{\text{irr}} > 600 \text{ nm}$ ) or blue-light ( $300 \text{ nm} < \gamma_{\text{irr}} < 560 \text{ nm}$ ) irradiation. The photoirradiation at room temperature was performed in the ESR cavity. The light intensity was  $3.0 \times 10^3 \text{ W m}^{-2}$  for both blue- and red-light irradiations at 77 K. The light was attenuated to  $\sim 50\%$  intensity in the ESR cavity.

ESR spectra were recorded on a Varian E-4 spectrometer with 100-kHz field modulation at 77 K and at room temperature. ESR power saturation measurements were performed on a Varian E-9 spectrometer with modulation frequencies at 100 kHz at 77 K and 270 Hz at 4.2 K. Electron spin echo spectra were recorded on a homebuilt spectrometer<sup>29</sup> at 4.2 K.

Optical absorption spectra were measured in a 1-mm path length quartz cell on a Perkin-Elmer Model 330 spectrophotometer at room temperature. With this spectrophotometer, the signal intensity of a reference sample was automatically subtracted from the signal intensity of the main sample. The vesicle solutions were diluted to  $1/6$  v/v with the buffer solution since the absorption intensities of Chla in the undiluted vesicle solutions were too strong to measure the absorbance. Beer's law was satisfied in the diluted vesicle solutions.

### Results

**Optical Absorption Spectra.** Figure 1 shows optical absorption spectra of Chla in diethyl ether and in liquid DPPC vesicle solutions with and without cholesterol at room temperature. Since there are no absorption peaks at 740 or 685 nm which are assigned to hydrated Chla polymer<sup>30a</sup> and aggregated Chla,<sup>30b</sup> respectively, Chla is solubilized in its monomeric form. The curved baselines of the spectra in the vesicle solutions result from light scattering by the vesicle suspension. Correction for the effect of the light

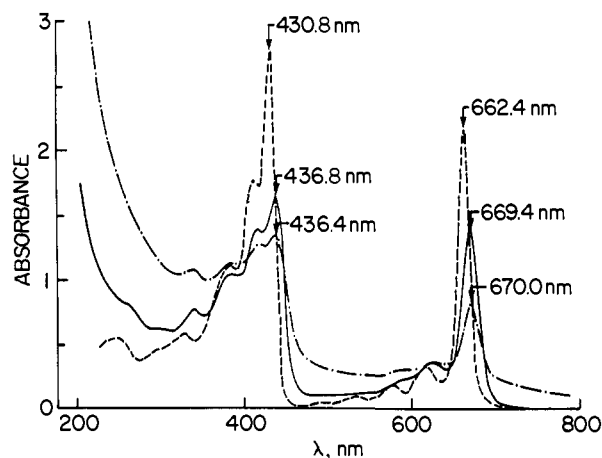


Figure 1. Optical absorption spectra of 0.25 mM Chla in a 1-mm pathlength quartz cell at room temperature: —, Chla in DPPC vesicle solution with no cholesterol (reference: water); - - -, Chla in DPPC vesicle solution with 50 mol % cholesterol (reference: water); - · - ·, Chla in diethyl ether (reference: diethyl ether). The vesicle solutions were diluted to  $1/6$  of the original vesicle solutions of 45 mM DPPC and 1.5 mM Chla.

scattering was done by subtracting the scattering component from the spectra shown in Figure 1. Ten times diluted vesicle solution gave ten times weaker absorption of Chla within experimental error. This indicates that the effect of multiple scattering is negligibly small and that no further correction for light scattering is needed. The red absorption band of Chla shows a red shift of  $7 \pm 1 \text{ nm}$  and a broadening of  $42 \pm 3\%$  in DPPC vesicle solutions compared to diethyl ether. The red peak absorption intensity, (peak height)  $\times$  (line width), of Chla in the vesicle solution with no cholesterol is  $92 \pm 3\%$  of that in diethyl ether although the overall concentration of Chla is the same.

Two effects of cholesterol addition on the Chla absorption are seen in Figure 1. First, the light scattering intensity increases. Second, the absorption intensity of Chla decreases. Since no change was observed in the red peak line width of Chla by cholesterol addition, the relative absorption intensity of Chla was measured from the peak height. In the vesicle solution containing 50 mol % cholesterol, the absorption intensity of Chla is  $42 \pm 3\%$  of that in diethyl ether.

The observed absorption intensities of Chla in the vesicle solutions, which are weaker than that in diethyl ether, are not explained by Duysens' "sieve effect".<sup>31</sup> The sieve effect explains a flattening of pigment absorption in large particles such as cells when the suspended particle diameters are significantly larger than the wavelength of the absorbed light. The inapplicability of Duysens' effect to small vesicles is shown as follows. First, this effect is only important when the transmission of light through a single suspended particle is substantially smaller than unity and the effect increases with the concentration of absorbing molecules. In the present case, assuming typical values of a vesicle radius of 10 nm and a lipid aggregation number of 2400,<sup>25</sup> the transmission of 669-nm light through a single vesicle is calculated to be 0.992 by using the value of molar extinction coefficient ( $8.63 \times 10^4 \text{ M}^{-1} \text{ cm}^{-1}$ ) of Chla at 660 nm in diethyl ether and our experimental concentrations of Chla (1.5 mM) and DPPC (45 mM). Second, Duysens' effect increases with the absorption per particle or the absorbing solute concentration per particle. However, our absorption correction is independent of the Chla concentration from 0.20 to 1.5 mM Chla. Third, Duysens' parameter  $\alpha_p$ , the absorbance of a single particle, implies that this parameter can be used to calculate the particle radius if the particle concentration of absorber and its extinction coefficient are known as discussed for spherical particles by Duysens.<sup>31</sup> From the data for our vesicle solution of Chla without cholesterol we obtain a calculated vesicle radius of 114 nm compared to the known value

(27) Strain, H. H.; Svec, W. A. In *The Chlorophylls*; Vernon, L. P., Seely, G. R., Eds.; Academic Press: New York, 1966; p 21.

(28) Oetmeier, W.; Norris, J. R.; Katz, J. J. *Z. Naturforsch., C: Biosci.* **1976**, *31C*, 163.

(29) Ichikawa, T.; Kevan, L.; Narayana, P. A.; *J. Phys. Chem.* **1979**, *83*, 3378.

(30) (a) Brown, R. G.; Evans, E. H. *Photochem. Photobiol.* **1980**, *32*, 103. (b) Lee, A. G. *Biochemistry*, **1975**, *14*, 4397.

(31) Duysens, L. N. M. *Biochim. Biophys. Acta* **1956**, *19*, 1.

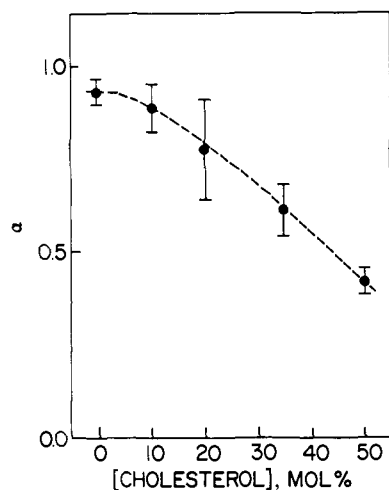


Figure 2. Dependence of the parameter  $\alpha$  for Chla on added cholesterol in liquid DPPC vesicle solution.

of about 10 nm. Thus, three different characteristics of small vesicle systems, (1) the absorption per vesicle, (2) the independence of the absorbance correction on the concentration of absorbing substance, and (3) the vesicle size, are inconsistent with Duysens' "sieve effect". Therefore, a different explanation must be considered.

The observed absorption intensities of Chla in the vesicle solutions can be explained by considering that the local light intensity is less inside the vesicles than outside, apparently due to scattering from the vesicle interface region. This is a different physical situation than scattering from an absorbing particle itself.

The light scattering from a vesicle surface can be understood in terms of Mie scattering from a small dielectric sphere with refractive index  $n_1$  immersed in a medium with a different refractive index  $n_2$ .<sup>32</sup> The light intensity inside the sphere is proportional to the square of the calculated electric field inside the sphere. For a sphere radius much less than the wavelength of the incident light, as applies to DPPC vesicles exposed to visible light, the ratio of the light intensity inside the sphere to that outside the sphere is  $(3/(n^2 + 2))^2$  where  $n = n_1/n_2$ . If we consider an alkane sphere in water,  $n \sim 1.1$  and the light intensity inside the sphere is about 0.9 of that outside the sphere. This is the correct magnitude for the empirical correction observed for Chla in DPPC vesicles. However, the larger corrections observed in the presence of cholesterol are larger than this idealized model predicts. A more detailed model for a vesicle which contains a water phase interior with refractive index  $n_2$  also gives the same result.

The larger corrections observed in the presence of cholesterol may be related to vesicle surface roughness and are discussed later. The absorbance correction for absorbing molecules solubilized within small particles such as vesicles which are smaller than the wavelength of the incident light can be calculated phenomenologically as follows. If a vesicle solution containing a light absorbing substance is illuminated by monochromatic light propagating in the  $x$  direction, the extinction of the light can be written as follows

$$dI(x)/dx = -\{\epsilon(\lambda)c\alpha I(x) + \beta(\lambda)I(x)\}/\log e \quad (1)$$

where  $I(x)$  is the light intensity outside the vesicle,  $\alpha I(x)$  the local light intensity at the site of the absorbing substance,  $\beta(\lambda)$  the light scattering efficiency at wavelength  $\lambda$ , and  $\epsilon(\lambda)$  and  $c$  are the molar extinction coefficient and the concentration of the absorbing substance, respectively. It should be noted in eq 1 that the absorbed energy by the absorbing substance is proportional to  $\alpha I(x)$  and not to  $I(x)$ . After the light has passed a vesicle solution of  $d$  cm pathlength, the total extinction is

$$\log(I_0/I) = \alpha\epsilon(\lambda)cd + \beta(\lambda)d \quad (2)$$

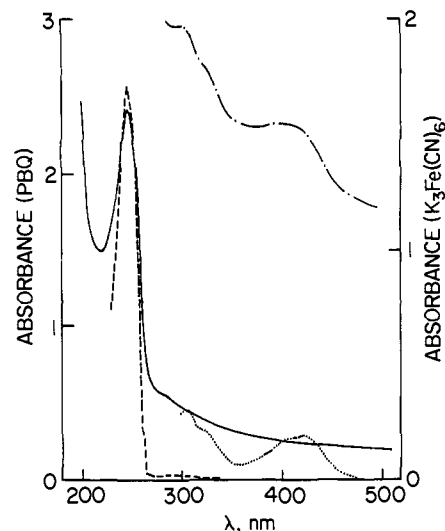


Figure 3. Optical absorption spectra of 1.2 mM PBQ and 1.7 mM  $K_3Fe(CN)_6$  in a 1-mm pathlength quartz cell at room temperature: —, PBQ in DPPC vesicle solution with no cholesterol (reference: water); ---, PBQ in chloroform (reference: chloroform); - · -,  $K_3Fe(CN)_6$  in DPPC vesicle solution with 50 mol % cholesterol (reference: water); ···,  $K_3Fe(CN)_6$  in water (reference: water). The vesicle solutions were diluted to  $1/6$  of the original vesicle solutions of 45 mM DPPC and 7 mM PBQ or 10 mM  $K_3Fe(CN)_6$ .

where  $I_0$  and  $I$  are the light intensities before and after the light passes through the sample.

We determine the correction  $\alpha$  for Chla absorption in vesicle solutions by comparison with the measured absorbance for Chla in diethyl ether solution where  $\alpha = 1$ . Figure 2 shows a plot of how  $\alpha$  varies with added cholesterol. The parameter  $\alpha$  decreases with cholesterol addition, and the effect is seen to be substantial. The  $\alpha$  correction was determined for all the vesicle solutions studied, and appropriate corrections were made for the determination of photoionization efficiency.

Figure 3 shows the optical absorption spectra of PBQ in chloroform and in DPPC vesicle solution with no cholesterol and shows the spectra of  $K_3Fe(CN)_6$  in water and in DPPC vesicle solution containing 50 mol % cholesterol at room temperature. PBQ has an absorption peak of 246 nm in chloroform. In the vesicle solution the absorption intensity of PBQ at 246 nm is  $\sim 60\%$  of that in chloroform. Although it is difficult to measure the total area of the absorption peak due to the strong light scattering in this wavelength region,  $\alpha < 1$  is apparent for PBQ in the vesicle solution in Figure 3. The absorption of  $K_3Fe(CN)_6$  in water vs. DPPC vesicles containing 50 mol % cholesterol shows a marked increase in the vesicle solution at 420 nm. However, the optical absorption intensity of  $K_3Fe(CN)_6$  at 420 nm in this vesicle solution is identical with that in water corresponding to  $\alpha = 1$ . This is as expected since  $K_3Fe(CN)_6$  is at the vesicle surface and in the bulk solution. This supports the interpretation of the apparent decreased absorbance for molecules solubilized within DPPC vesicles.

**Photoionization Yields.** Blue- and red-light irradiations were carried out on frozen DPPC vesicle solutions at 77 K and on liquid DPPC vesicle solutions at room temperature. The yields of photoinduced paramagnetic products were detected by ESR. The average yields of two or four experiments are plotted with error bars showing the extremes observed.

**No Electron Scavenger.** In the DPPC vesicle solution with no electron scavenger, only a negligibly weak ESR singlet was observed in the  $g = 2.002$  region during and after both blue- and red-light irradiations at room temperature, as reported previously.<sup>26,28,33</sup> At 77 K, on the other hand, a symmetric single ESR line was observed after both blue- and red-light irradiations at  $g = 2.0026 \pm 0.0004$  with a line width of  $10 \pm 1$  G as shown in

(32) Born, M.; Wolf, E. In *Principles of Optics*; Pergamon Press: Oxford, 1964; Chapter 13.

(33) Tomkiewicz, M.; Corker, G. A. *Photochem. Photobiol.* 1975, 22, 249.

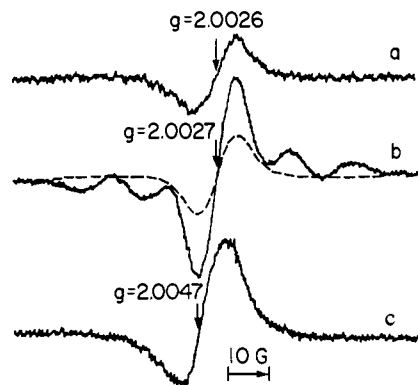


**Figure 4.** ESR spectra of frozen DPPC (45 mM) vesicle solutions of Chla containing 50 mol % cholesterol (a) with no electron scavenger, (b) with  $K_3Fe(CN)_6$ , and (c) with PBQ after 2-h blue-light irradiation at 77 K. The broken line in (b) is the spectra before photoirradiation. Added amounts of Chla, PBQ, and  $K_3Fe(CN)_6$  were 1.5, 7, and 10 mM, respectively.

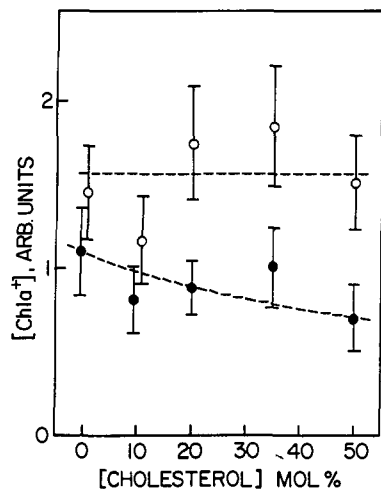


**Figure 5.** Dependence of  $Chla^+$  yield on added cholesterol concentration after 2-h blue- (O) and red- (●) light irradiations of frozen DPPC 45 mM vesicle solution with 1.5 mM Chla but no electron scavenger at 77 K.

Figure 4a. This ESR singlet has been assigned to  $Chla^+$  by Ohta and Kevan.<sup>26</sup>

The photoionization yields of Chla after 2-h blue- and red-light irradiations at 77 K were measured from the ESR signal intensity of  $Chla^+$  and are shown in Figure 5 vs. added cholesterol after the  $\alpha$  correction for the local light intensity of Chla inside the vesicles. In Figure 5 the photoionization yield by red-light irradiation decreases to  $\sim 70\%$  with 50 mol % cholesterol addition. In the case of blue-light irradiation, on the other hand, no obvious cholesterol effect is seen. With no Chla but with 50 mol % cholesterol in the vesicle solution, radical formation was observed by blue-light irradiation at 77 K in the  $g = 2.002$  region with an ESR intensity about  $\sim 20\%$  of the  $Chla^+$  signal, while no radical formation was observed by red-light irradiation. The apparent photoionization yield of Chla by blue-light irradiation in Figure 5 may have been affected by this background radical formation to mask a possible trend with added cholesterol.

**PBQ as Electron Scavenger.** In DPPC vesicle solution with 7 mM PBQ as an electron scavenger a weak quintet ESR signal was observed before photoirradiation at room temperature. This "dark" signal is not generated by fluorescent room light, and its origin is unclear. After exposure to blue or red light at room temperature, the signal intensity of this quintet increased and reached a stationary value within 1 s. After the light was turned off, the signal intensity decreased and reached a stationary value within a few seconds. After turning on the light again, the signal intensity increased to the same stationary value as before. The ESR signals in these stationary states after turning on and off

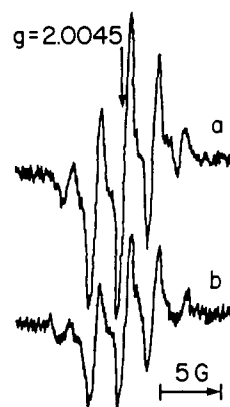


**Figure 6.** ESR spectra of  $PBQ^-$  at room temperature at stationary state after turning on (a) and off (b) red-light irradiation in liquid DPPC (45 mM) vesicle solution containing Chla and PBQ. Added amounts of Chla and PBQ were 1.5 and 7 mM, respectively.

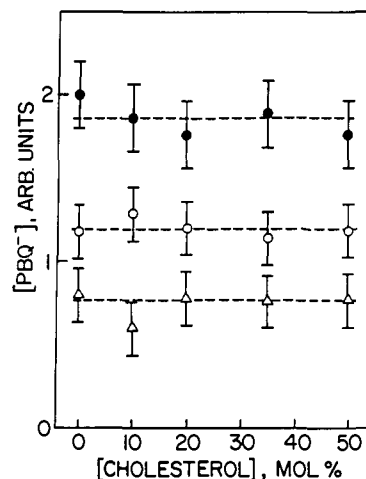


**Figure 7.** Dependence of  $PBQ^-$  yields on added cholesterol concentration at stationary state after turning on (●) and off (○) red-light irradiation at room temperature and the difference of these two (Δ) in liquid DPPC (45 mM) vesicle solution with Chla and PBQ. Added amounts of Chla and PBQ were 1.5 and 7 mM, respectively.

the light are shown in Figure 6. These quintet signals are characterized by  $g = 2.0045$  and a splitting of 2.2 G and can be assigned to  $PBQ^-$  anion radical ( $PBQ^-$ ).<sup>28,34</sup> Without Chla in the system, no increase in the  $PBQ^-$  signal intensity was observed after exposure to blue or red light. This indicates that the increase after turning on the light shown in Figure 6 is due to electron transfer from photoexcited Chla to  $PBQ^-$ . The formation of  $Chla^+$  was not observed at room temperature for unknown reasons as reported previously,<sup>28,34</sup> possibly  $Chla^+$  decays rapidly at room temperature or reduced quinone impurity is present which removes  $Chla^+$ .

The two stationary signal intensities of  $PBQ^-$  at room temperature after turning on and off the light and the difference of these two were measured as a function of added cholesterol concentrations. They are shown in Figure 7 for the case of red-light irradiation after correction to the local light intensity at Chla. In Figure 7 no cholesterol effect is seen on the signal intensities of  $PBQ^-$ . The same was true for blue-light irradiation.

At 77 K, no ESR signal was observed before photoirradiation. After blue-light irradiation at 77 K, an asymmetric singlet ESR signal with a line width of  $11 \pm 1$  G was observed at  $g = 2.0047 \pm 0.0004$  as shown in Figure 4c. Even without Chla in the system, a similar ESR singlet with a similar intensity was observed at  $g = 2.0052 \pm 0.0003$  after blue-light irradiation at 77 K. This indicates that the asymmetric singlet is the signal of a  $PBQ^-$  radical produced by direct photoexcitation of  $PBQ^-$ . In fact,  $PBQ^-$  has a weak absorption band in the blue-light region. A similar asym-

(34) Tollin, G.; Green, G. *Biochim. Biophys. Acta* **1962**, *60*, 524.

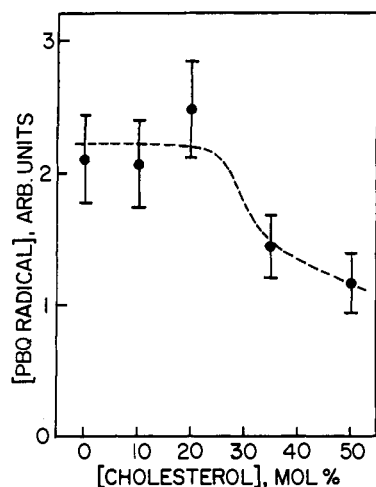


**Figure 8.** Dependence of PBQ radical yield on added cholesterol concentration after 2-h blue-light irradiation at 77 K in frozen DPPC (45 mM) vesicle solution with Chla and PBQ. Added amounts of Chla and PBQ were 1.5 and 7 mM, respectively.

metric singlet was also observed at  $g = 2.0057$  after blue-light irradiation of PBQ at 77 K in ethanol, but in benzene a symmetric singlet ESR signal with a line width of 16.0 G was observed at  $g = 2.0040$  after blue-light irradiation.

The PBQ radical yield after 2-h blue-light irradiation of the vesicle solution with Chla and PBQ at 77 K was measured from the ESR signal intensity and is shown in Figure 8 vs. added cholesterol concentration after correction for the local light intensity at PBQ. In Figure 8 the radical yield decreases when the cholesterol concentration exceeds 25 mol %. A similar cholesterol effect on the PBQ radical yield is observed in the vesicle solution without Chla.

After red-light irradiation of vesicles containing Chla at 77 K, a very weak ESR signal with a line width of 7 G was observed. The ESR intensity was ten times weaker than that of the PBQ radical after blue-light irradiation. Without Chla, no ESR signal was observed after red-light irradiation, so that the observed radical formation is probably due to charge transfer from photoexcited Chla to PBQ. Similar radical formation has been reported in an ether-isopentane-ethanol mixture (8:3:5 v/v) at  $-135^\circ\text{C}$ .<sup>34</sup> When cholesterol was added to the vesicle, however, some other radical signal overlapped with the PBQ radical signal produced by the red-light irradiation to hide the latter.

**$\text{K}_3\text{Fe}(\text{CN})_6$  as Electron Scavenger.** In DPPC vesicle solution with 10 mM  $\text{K}_3\text{Fe}(\text{CN})_6$  as an electron scavenger, no radical formation was observed at room temperature during and after blue- and red-light irradiations.<sup>28,33</sup> At 77 K, an ESR signal of  $\text{Chla}^+$  was observed even before photoirradiation as seen in Figure 4b. By blue- and red-light irradiations at 77 K, the signal intensity increased. In the case of no cholesterol in the vesicle, the signal intensities of  $\text{Chla}^+$  after 2-h blue- and red-light irradiations were four and eight times stronger, respectively, than those in the vesicle solution with no electron scavenger. This indicates that the  $\text{Chla}^+$  formation in this system is due to electron transfer from excited Chla to ferricyanide ions ( $\text{Fe}(\text{CN})_6^{3-}$ ). The apparent smaller electron-transfer efficiency by blue-light irradiation is due to the existence of an absorption band of  $\text{Fe}(\text{CN})_6^{3-}$  at 420 nm as shown in Figure 3.<sup>26</sup> After blue-light irradiation of the vesicle solution containing cholesterol at 77 K, a quintet ESR signal with a splitting of 16 G was observed overlapping with the  $\text{Chla}^+$  signal as shown in Figure 4b. This quintet signal was observed even without Chla in the system, so that this radical formation seems to originate from the photoexcitation of  $\text{Fe}(\text{CN})_6^{3-}$  in its 420-nm absorption band.

The photoionization yields of Chla by 2-h blue- and red-light irradiations at 77 K were measured from the increase in the signal intensity of  $\text{Chla}^+$  by the irradiation and are shown in Figure 9 vs. added cholesterol concentration after correction to the local light intensity at Chla. The photoionization yields of Chla with

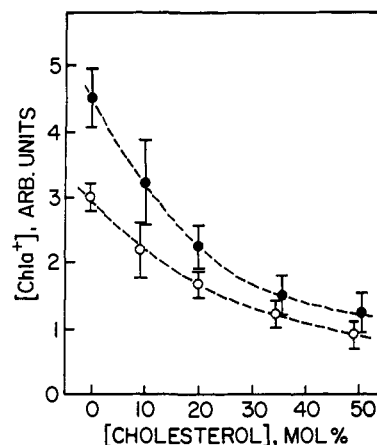


**Figure 9.** Dependence of  $\text{Chla}^+$  yields on added cholesterol concentration after 2-h blue- (O) and red- (●) light irradiation at 77 K in frozen DPPC (45 mM) vesicle solution with Chla and  $\text{K}_3\text{Fe}(\text{CN})_6$ . Added amounts of Chla and  $\text{K}_3\text{Fe}(\text{CN})_6$  were 1.5 and 10 mM, respectively.

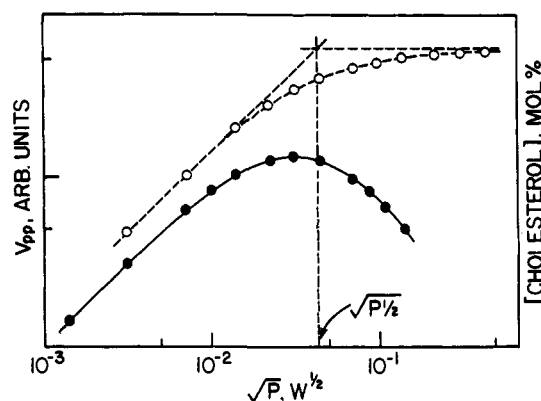


**Figure 10.** ESR power saturation curves of  $\text{Chla}^+$  at 77 K (O) and 4 K (●) in frozen DPPC (45 mM) vesicle solution containing  $\text{K}_3\text{Fe}(\text{CN})_6$  after 2-h red-light irradiation at 77 K. Added amounts of Chla and  $\text{K}_3\text{Fe}(\text{CN})_6$  were 1.5 and 10 mM, respectively. The solid line is a theoretical fit to the Castner-Zhidkov equation.

red light are the most accurate and show a monotonic decrease with cholesterol addition. Since the addition of 10 mM  $\text{K}_3\text{Fe}(\text{CN})_6$  significantly increased the turbidity as shown in Figure 3, the photoionization yield of Chla was also measured in DPPC vesicle solution with the lower concentration of 2 mM  $\text{K}_3\text{Fe}(\text{CN})_6$ . The same decrease in Chla photoionization efficiency was observed.

**Paramagnetic Relaxation Times of  $\text{Chla}^+$ .** ESR power saturation measurements for  $\text{Chla}^+$  in frozen DPPC vesicle solutions with 10 mM  $\text{K}_3\text{Fe}(\text{CN})_6$  were carried out at 77 K and 4.2 K by measuring the peak-to-peak signal intensity of  $\text{Chla}^+$  as a function of incident microwave power. Since the sample loaded cavity  $Q$  is constant, the square root of the incident microwave power is proportional to the microwave magnetic field  $H_1$  at the sample.<sup>35</sup> Typical saturation curves are shown in Figure 10. At 77 K, saturation occurred in the maximum microwave power region of the ESR spectrometer. From the saturation curves at 77 K, relative values of  $(T_1T_2)^{1/2}$  for different cholesterol concentrations were estimated by using the following relation

$$(P_{1/2})^{1/2} \propto 1/(T_1T_2)^{1/2} \quad (3)$$

where  $T_1$  and  $T_2$  are the longitudinal and transverse relaxation times of  $\text{Chla}^+$ , respectively, and  $P_{1/2}$  is the microwave power at the intersection of two tangents from the unsaturated region and from the maximum point of the saturation curve as shown in Figure 10. The value of  $P_{1/2}$  as a function of cholesterol concentration is shown in Figure 11. In Figure 11  $P_{1/2}$ , and so

(35) Poole, C. P. In *Electron Spin Resonance*; Wiley-Interscience: New York, 1967; pp 291, 710.

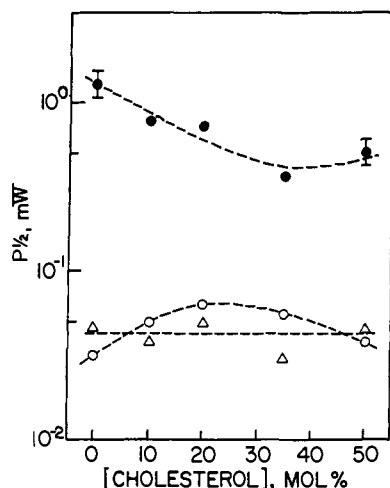


**Figure 11.** Dependence of the saturation parameter  $P_{1/2}$  at 77 K on added cholesterol concentration for Chla<sup>+</sup> in frozen DPPC vesicle solutions with  $\text{K}_3\text{Fe}(\text{CN})_6$  ( $\bullet$ ) and with no electron scavenger ( $\circ$ ) and for PBQ radical ( $\Delta$ ) in frozen DPPC vesicle solution with Chla.  $P_{1/2}$  is proportional to  $(T_1 T_2)^{-1}$ .

$(T_1 T_2)^{-1}$ , decreases with an increase in cholesterol concentration in vesicle solutions with 10 mM  $\text{K}_3\text{Fe}(\text{CN})_6$ . Similar cholesterol effects on the relaxation times of Chla<sup>+</sup> were observed in vesicle solutions with the lower concentration of 2 mM  $\text{K}_3\text{Fe}(\text{CN})_6$ .

ESR power saturation measurements were carried out at 77 K for Chla<sup>+</sup> in a DPPC vesicle solution without an electron scavenger and for the PBQ radical produced by blue-light irradiation in a DPPC vesicle solution containing Chla. The values of  $P_{1/2}$  in these cases vs. cholesterol concentration are shown in Figure 11 for comparison. It is seen in Figure 11 that the relaxation times of Chla<sup>+</sup> become more than ten times shorter in the presence of  $\text{Fe}(\text{CN})_6^{3-}$ , as reported previously.<sup>26</sup> The relaxation times of Chla<sup>+</sup> in the presence of  $\text{Fe}(\text{CN})_6^{3-}$  were not affected by dipolar interaction with other Chla<sup>+</sup>, because no difference was seen in the relaxation times of Chla<sup>+</sup> between two samples irradiated for 10 min and 2 h, the ratio of the Chla<sup>+</sup> concentrations being 1:3. These results indicate that when the vesicle solution contains  $\text{Fe}(\text{CN})_6^{3-}$ , the relaxation time of Chla<sup>+</sup>, especially  $T_2$ , is determined by the paramagnetic dipolar interaction between Chla<sup>+</sup> and  $\text{Fe}(\text{CN})_6^{3-}$ .

At 4 K, power saturation occurred at lower microwave power, and the saturation curve shape changed. The saturation curve at 4 K could be analyzed by the Castner-Zhidkov theoretical analysis.<sup>36-39</sup> This analysis is for the saturation of inhomogeneously broadened ESR lines and is based on a noninteracting spin packet model. The ESR line of Chla<sup>+</sup> is inhomogeneously broadened by unresolved hyperfine interaction with the ring protons.<sup>40</sup> The fits to the saturation curves are shown in Figure 10, the detailed procedure of which is described in the original papers.<sup>36,37</sup> This analysis gives separate values for  $T_1$  and  $T_2$  which are shown in Figure 12 as a function of cholesterol concentration. The trends of  $T_1$  and  $T_2$  with cholesterol concentration are considered reliable although the absolute values are probably not, due to some deviation from the noninteracting spin packet assumption in the analysis. In particular, the increased ESR line width with saturation is not quantitatively accounted for by the Castner-Zhidkov analysis which can be related to some spin packet interaction. The reliability of the relative values of  $T_1$  and  $T_2$  obtained by this analysis has been well demonstrated in the course

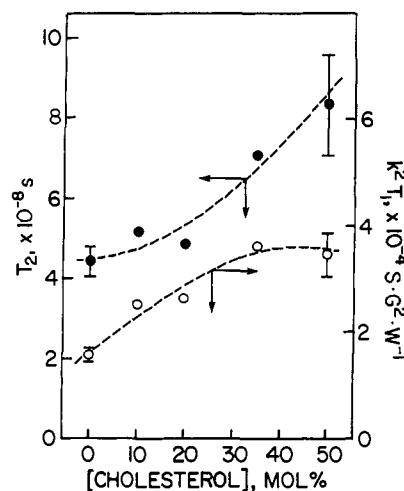


**Figure 12.** Dependence of paramagnetic relaxation times  $T_1$  ( $\circ$ ) and  $T_2$  ( $\bullet$ ) of Chla<sup>+</sup> at 4 K on added cholesterol in frozen DPPC vesicle solution with  $\text{K}_3\text{Fe}(\text{CN})_6$ . The constant  $k$  determines the relation between the microwave magnetic field  $H_1$  (G) at the sample inside the ESR cavity and the incident microwave power  $P$  (W) into the cavity according to:  $H_1 = k(P)^{1/2}$ .

of determining relative distances between radiation-produced paramagnetic species.<sup>41-43</sup>

The trend of  $T_2$  with cholesterol can be qualitatively checked independently by two pulse electron spin echo measurements of the phase memory time which is related to the transverse relaxation time. Spin echo measurements at 4.2 K showed that the phase memory time of Chla<sup>+</sup> was shorter than the 100 ns dead time of our electron spin echo instrument so that only the tail of the relaxation trace was observed. Comparing the two cases of 0 mol % and 50 mol % cholesterol, the echo intensity was stronger in the case of 50 mol % cholesterol although the ESR signal intensity was two times weaker in this case. This indicates that the phase memory time and consequently  $T_2$  of Chla<sup>+</sup> is longer in the case of 50 mol % cholesterol. Thus, the electron spin echo results qualitatively support the  $T_2$  trend from the ESR saturation analysis.

## Discussion

**Local Light Intensity Inside the Vesicle Bilayer.** There is a substantial difference between the  $\alpha$  factors for Chla and PBQ vs.  $\text{Fe}(\text{CN})_6^{3-}$  in liquid DPPC vesicle solutions. The value of  $\alpha = 1$  for  $\text{Fe}(\text{CN})_6^{3-}$  is understood on the basis that  $\text{Fe}(\text{CN})_6^{3-}$  does not penetrate the vesicle surface significantly since it is highly charged and hydrophilic. Chla is clearly solubilized by the DPPC vesicle, but most evidence suggests that it is located near the vesicle bilayer surface.<sup>9,26,28,44-46</sup> On the other hand, neutral quinones are expected to penetrate more completely into the vesicle bilayer.<sup>6,47</sup> Values of  $\alpha < 1$  for Chla and PBQ indicated that the local light intensity inside the vesicle bilayer is lower than outside.

Added cholesterol to DPPC vesicles causes structural changes at the interface and within the vesicles.<sup>48</sup> The specifics of these structural changes have been described as intercalation of cholesterol near the headgroup region to increase the separation of the headgroups of the phospholipids<sup>49a</sup> and as an increase in the internal fluidity of the vesicle bilayers below their phase transitions.<sup>24,49b</sup> The vesicle size also increases<sup>50</sup> as is also shown here

(41) Lin, D. P.; Kevan, L. *J. Chem. Phys.* **1971**, *55*, 2629.

(42) Zimbrick, J.; Kevan, L. *J. Chem. Phys.* **1967**, *47*, 2364.

(43) Salikhov, K. M.; Tsvetkov, Yu. D. In *Time Domain Electron Spin Resonance*; Kevan, L., Schwartz, R. N., Eds.; Wiley-Interscience: New York, 1979; p 231.

(44) Hurlley, J. K.; Tollin, G. *Sol. Energy* **1982**, *28*, 187.

(45) Fünfschilling, J.; Waltz, D. *Photochem. Photobiol.* **1983**, *38*, 389.

(46) Ohta, N.; Narayana, M.; Kevan, L. *J. Chem. Phys.* **1985**, *83*, 4382.

(47) Ford, W. E.; Tollin, G. *Photochem. Photobiol.* **1984**, *40*, 249.

(48) *Membrane Fluidity in Biology*; Aloia, R. C., Ed.; Academic Press: New York, 1983; Vol. 2, pp 15-18, 176-179, 254.

(49) (a) Yeagle, P. L. *Acc. Chem. Res.* **1978**, *11*, 321. (b) Shreier-Muccillo, S.; Marsh, D.; Dugas, H.; Schneider, H.; Smith, I. C. P. *Chem. Phys. Lipids* **1973**, *10*, 11.

(36) Castner, T. G. *Phys. Rev.* **1959**, *115*, 1506.

(37) Zhidkov, O. P.; Muromtsev, V. I.; Akhvediani, I. G.; Safronov, S. N.; Kopylov, V. V. *Sov. Phys. Solid State* **1967**, *9*, 1095.

(38) Hase, H.; Higashimura, T.; Hiromitsu, I. *J. Phys. Chem.* **1982**, *86*, 3333.

(39) Hiromitsu, I.; Hase, H.; Higashimura, T. *Jp. J. Appl. Phys.* **1985**, *24*, 704.

(40) Borg, D. C.; Fajer, J.; Felton, R. H.; Dolphin, D. *Proc. Natl. Acad. Sci. U.S.A.* **1970**, *67*, 813.

by the enhancement of light scattering by cholesterol addition in Figure 1. These structural effects must be responsible for the monotonic decrease in the  $\alpha$  value for Chla as a function of added cholesterol in Figure 2. The dominant structural effects responsible for this are probably the increases in the vesicle diameter by 30–40 % at 50 mol % cholesterol<sup>50</sup> and in the separation of the headgroups. Although the vesicle diameter increases, it is still far less than the wavelength of the irradiation light, and under this condition Mie scattering is independent of particle size. However, the increased headgroup separation due to cholesterol intercalation may increase the vesicle surface roughness to enhance the light scattering and decrease the penetrating light intensity within the vesicle.

**Solubilization Site and Photoionization Efficiency of Chla.** In the frozen DPPC vesicle solution with  $K_3Fe(CN)_6$ , the paramagnetic relaxation time of  $Chla^+$ , especially  $T_2$ , is determined by the paramagnetic dipolar interaction between  $Chla^+$  and  $Fe(CN)_6^{3-}$ . When cholesterol was added into the solution,  $T_2$  became longer as shown in Figure 12. This indicates that the mean distance between  $Chla^+$  and  $Fe(CN)_6^{3-}$  increases and that the dipolar interaction becomes weaker with cholesterol addition. Although the absolute value of  $T_2$  derived from the saturation data is rather uncertain, it is interesting to calculate an interaction distance from the following relation.<sup>51,52</sup>

$$r \text{ (cm)} \approx 1 \times 10^{-4} [T_2 \text{ (s)}]^{1/3} \quad (4)$$

The relation between  $T_2$  and the local spin density in single crystals, polycrystals, and glasses has been satisfactorily explained with this equation.<sup>51,52</sup> The approximate distances at 0 and 50 mol % cholesterol are 3.5 and 4.2 nm. These seem too large, but the 20 % average distance increase is perhaps reasonable. The qualitative increase in the average distance between  $Chla^+$  and  $Fe(CN)_6^{3-}$  with cholesterol addition is interpreted by Chla moving deeper into the vesicle while  $Fe(CN)_6^{3-}$  remains near the vesicle surface. The deeper average penetration of Chla may be caused by the increased internal fluidity of alkyl chain straightening of the bilayer in the presence of cholesterol.

In the present photoionization study, by adding 50 mol % cholesterol, the photoionization efficiency of Chla at 77 K decreased by ~30% in the DPPC vesicle solution with no electron scavenger and by ~70% in the DPPC vesicle solution with  $K_3Fe(CN)_6$  as an electron scavenger. In contrast, the electron-transfer efficiency from the photoexcited Chla to PBQ electron scavenger was not affected by cholesterol addition at room temperature. The correlation in structure between liquid and frozen micellar and vesicular systems has been shown elsewhere.<sup>4,20,53</sup> The decrease in the case of  $K_3Fe(CN)_6$  as an electron scavenger correlates well with the distance increase between  $Chla^+$  and  $Fe(CN)_6^{3-}$  observed by the relaxation measurement of  $Chla^+$ . With no electron scavenger, the photoionization efficiency of Chla is assumed to be determined by the interaction distance between Chla and water molecules since initial hydration of the photoexcited electron is essential for charge separation in this system.<sup>1</sup> The decrease in the photoionization efficiency of Chla with the

cholesterol addition is explained by a deeper solubilization site of Chla in the vesicle which causes a longer interaction distance between Chla and water at the vesicle surface.

With PBQ as electron acceptor, no effect of cholesterol on the photoionization efficiency was seen. The interpretation is that PBQ is inside the vesicle and moves deeper into the vesicle bilayer when cholesterol is added as does Chla so that their average interaction distance does not change. The decrease in the direct photodissociation efficiency of PBQ with cholesterol addition shown in Figure 8 supports this interpretation. The decrease may be explained by the longer interaction distance between PBQ and water. It is concluded that both Chla and PBQ move deeper into the vesicle bilayer when cholesterol is added because of the increase in the fluidity inside the bilayer.<sup>24</sup> Thus cholesterol can be used to control the Chla photoionization efficiency to a limited degree dependent upon the nature of the electron scavenger.

The present result on the cholesterol effect on the solubilization site of Chla contrasts with recent results of Ford and Tollin in egg yolk phosphatidylcholine vesicle solutions.<sup>47</sup> They concluded that Chla molecules become more accessible to water and to  $Fe(CN)_6^{3-}$  by cholesterol addition. The difference may be attributed to a different role of cholesterol in the egg yolk phosphatidylcholine vesicles due to the existence of unsaturated bonding in the hydrocarbon chains. Indeed, electron spin probe studies show a distinct difference in cholesterol effects on the alkyl chain motional amplitudes in egg yolk vs. dipalmitoylphosphatidylcholine vesicles<sup>48</sup> which is apparently due to the double bond in the alkyl chain of egg yolk phosphatidylcholine.<sup>24</sup>

## Conclusions

Optical absorption studies of Chla, PBQ, and  $K_3Fe(CN)_6$  in liquid DPPC vesicle solutions show that correction for the light intensity inside the vesicle must be made. A decrease in the optical absorption intensity of Chla by cholesterol addition is explained by increases in the vesicle size and by the separation of the phospholipid headgroups to cause a weaker light intensity inside the vesicle.

The results of ESR power saturation measurements of  $Chla^+$  in frozen DPPC vesicle solution with added  $K_3Fe(CN)_6$  show that the mean distance between  $Chla^+$  and  $Fe(CN)_6^{3-}$  increases with 50 mol % cholesterol addition. Electron spin echo measurements support the ESR power saturation result. The observed distance increase between  $Chla^+$  and  $Fe(CN)_6^{3-}$  gives evidence that the porphyrin ring of Chla sitting near the lipid headgroup moves deeper into the vesicle bilayer with added cholesterol.

The photoionization efficiency of Chla at 77 K with no electron scavenger decreases ~30% with 50 mol % cholesterol addition. In contrast, the electron-transfer efficiency from excited Chla to the PBQ electron scavenger is not affected by added cholesterol at room temperature; while, with  $K_3Fe(CN)_6$  the electron-transfer efficiency decreases by ~70% at 77 K with 50 mol % cholesterol addition. It is concluded that both Chla and PBQ move deeper into the vesicle bilayer when cholesterol is added because of an increase in the fluidity or the alkyl chain straightening inside the bilayer.

**Acknowledgment.** This research was supported by the Department of Energy, Office of Basic Energy Sciences. We are grateful to Dr. N. Ohta for providing information about vesicle preparation.

(50) (a) deKruijff, B.; Cullis, P. R.; Radda, G. K. *Biochim. Biophys. Acta* **1976**, *436*, 729. (b) Johnson, S. M. *Biochim. Biophys. Acta* **1973**, *307*, 27.

(51) Kittel, C.; Abrahams, E. *Phys. Rev.* **1954**, *90*, 238.

(52) Wyard, S. J. *Proc. Phys. Soc. London* **1965**, *86A*, 587.

(53) Bales, B. L.; Kevan, L. *J. Phys. Chem.* **1982**, *86*, 3836.